PISTON
Journal of Technical Engineering:

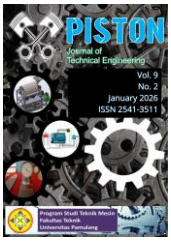

Synthesis and Characterization of Dual-doped (Al, Co) ZnO Nanofibers for Sustainable Piezoelectric Nanogenerator Applications

Ade Irvan Tauvana[1,a)], Lukman Nulhakim[1], Elsa Nurfadillah[1]

[1]*Department of Manufacturing Engineering Technology, Politeknik Enjinering Indorama, Purwakarta 41152, Indonesia*

E-mail: [a)] ade.irvan@pei.ac.id

Received: September 10, 2025 *Revision: January 20, 2026* *Accepted: January 29, 2026*

Abstract: This study reports the structural and morphological enhancement of aluminum (Al) and cobalt (Co) co-doped ZnO nanofibers synthesized via electrospinning for piezoelectric applications. The morphology and elemental composition were systematically analyzed using Scanning Electron Microscopy coupled with Energy-Dispersive X-ray Spectroscopy (SEM–EDX), while crystallographic properties were evaluated by X-ray Diffraction (XRD). SEM analysis revealed that the electrospun Al–Co co-doped ZnO nanofibers formed a highly interconnected and porous fibrous network with a uniform diameter distribution and negligible agglomeration, exhibiting diameters of 100–200 nm. EDX results confirmed the successful incorporation of Al and Co dopants into the ZnO matrix without detectable impurities. XRD patterns indicated a well-defined hexagonal wurtzite crystal structure with high crystallinity and a pronounced preferred orientation. The crystallite size, calculated using the Scherrer equation, ranges from 84 to 106 nm. The variation in crystallite size among different diffraction peaks is mainly attributed to differences in peak broadening (FWHM), which may indicate anisotropic crystallite growth and varying degrees of lattice orderingIn addition, the microstrain increased from 1.5×10^{-4} to 3.8×10^{-4}, suggesting lattice distortion induced by Al^{3+} and Co^{2+} substitution. These findings demonstrate that Al–Co co-doped ZnO nanofibers possess favorable structural characteristics for advanced piezoelectric material development.

Keywords: Electrospun ZnO Nanofibers, SEM–EDX, XRD, Crystallite Size; Microstrain, Piezoelectric Materials.

Abstrak: *Penelitian ini bertujuan untuk menganalisis karakteristik morfologi, komposisi unsur, dan struktur kristal nanofiber ZnO terdoping aluminium (Al) dan kobalt (Co) yang disintesis menggunakan metode elektrospinning. Karakterisasi morfologi dan distribusi unsur dilakukan menggunakan Scanning Electron Microscopy–Energy-Dispersive X-ray Spectroscopy (SEM–EDX), sedangkan sifat struktur kristal dianalisis menggunakan X-ray Diffraction (XRD). Hasil SEM menunjukkan bahwa nanofiber ZnO terdoping Al–Co membentuk jaringan serat berpori yang saling berjalin, terdistribusi homogen tanpa aglomerasi signifikan, dengan diameter nanofiber berkisar antara 100–200 nm. Analisis EDX mengonfirmasi keberadaan unsur O, Zn, Al, dan Co tanpa terdeteksinya unsur pengotor, yang menunjukkan kemurnian material yang relatif baik serta keberhasilan proses doping. Pola XRD memperlihatkan struktur kristal heksagonal wurtzite dengan tingkat kristalinitas yang baik dan orientasi kristal dominan. Ukuran kristalit yang dihitung menggunakan persamaan Scherrer berada pada rentang 84–106 nm dan menunjukkan tren meningkat pada puncak difraksi dengan nilai 2θ yang lebih tinggi. Nilai regangan mikro (microstrain) meningkat dari $1,5 \times 10^{-4}$ hingga $3,8 \times 10^{-4}$, yang mengindikasikan adanya distorsi kisi akibat substitusi ion Al^{3+} dan Co^{2+}. Karakteristik tersebut menunjukkan potensi nanofiber ZnO terdoping Al–Co untuk aplikasi piezoelektrik.*

Kata kunci: *ZnO Nanofiber; SEM–EDX; XRD; Ukuran Kristalit; Microstrain; Piezoelektrik.*

INTRODUCTION

Zinc oxide (ZnO) is a II–VI semiconductor that has attracted considerable research interest due to its wide direct bandgap of approximately 3.37 eV and high exciton binding energy of around 60 meV at room temperature. These intrinsic characteristics make ZnO a promising material for various applications, including optoelectronics, sensors, photocatalysis, and piezoelectric energy harvesting systems [1], [2]. Among these properties, the piezoelectric behavior of ZnO is particularly significant for nanogenerator applications, where

ambient mechanical energy can be converted into electrical energy to support self-powered and sustainable electronic devices [3].

ZnO nanostructures such as nanowires, nanorods, nanotubes, and nanofibers exhibit enhanced piezoelectric responses compared to bulk ZnO due to their high surface-to-volume ratio, superior mechanical flexibility, and efficient stress-induced polarization [4], [5]. These characteristics allow ZnO-based nanogenerators to operate effectively under low-frequency and low-amplitude mechanical excitations, which are commonly encountered in real-world environments [6]. In particular, one-dimensional ZnO nanofibers offer additional advantages, including continuous charge transport pathways and improved mechanical durability, making them highly suitable for flexible and wearable energy harvesting devices [7].

Despite these advantages, pristine ZnO still suffers from several inherent limitations, such as weak polarization strength, low carrier mobility, and defect-induced charge recombination caused by oxygen vacancies and zinc interstitials [8]. These drawbacks significantly limit the energy conversion efficiency and long-term stability of ZnO-based piezoelectric nanogenerators. To overcome these challenges, various material engineering strategies have been explored, among which metal-ion doping has emerged as one of the most effective approaches to tailor the structural, electrical, and piezoelectric properties of ZnO [9].

Among various dopants, aluminum (Al) and cobalt (Co) have received considerable attention due to their distinct and complementary effects on ZnO. Al^{3+} doping, which involves the substitution of Zn^{2+} ions, has been reported to improve crystallinity, increase carrier concentration, and reduce grain boundary resistance, thereby enhancing electrical conductivity and piezoelectric output [10]. In contrast, Co^{2+}/Co^{3+} doping can induce lattice distortion and modify the electronic band structure of ZnO, which may contribute to improved polarization-related behavior in piezoelectric applications [11]. However, single-element doping often results in trade-offs between electrical performance, crystallinity, and mechanical stability.

Recent studies have demonstrated that co-doping strategies can provide synergistic enhancements by combining the advantages of different dopant elements while mitigating their individual limitations [12]. In particular, Al–Co dual-doped ZnO has been reported to exhibit improved crystallinity, controlled defect states, enhanced lattice strain, and superior piezoelectric performance compared to singly doped or undoped ZnO [13]. Such synergistic effects are especially important for sustainable and flexible energy harvesting systems, where high electrical output and mechanical robustness are both critical requirements.

Electrospinning is a simple, scalable, and cost-effective fabrication technique that enables the production of continuous one-dimensional nanofibers with controlled diameter, high porosity, and homogeneous dopant distribution [14]. Electrospun ZnO nanofibers offer a porous network structure that facilitates efficient stress transfer and enhances piezoelectric response, making them promising candidates for next-generation sustainable piezoelectric nanogenerators [15]. Furthermore, electrospinning is compatible with large-area and flexible substrates, supporting its potential for practical device applications.

In this study, dual-doped (Al, Co) ZnO nanofibers were synthesized using the electrospinning method followed by thermal treatment to obtain crystalline ZnO structures. The effects of Al–Co co-doping on the morphological characteristics, crystallinity, and fiber diameter were systematically investigated using scanning electron microscopy (SEM) and X-ray diffraction (XRD). This work aims to provide a deeper understanding of the structure–property relationships of dual-doped ZnO nanofibers and to support the development of high-performance and sustainable piezoelectric nanogenerators for future self-powered systems.

METHODS

Zinc acetate dihydrate ($Zn(CH_3COO)_2 \cdot 2H_2O$, Merck), cobalt acetate tetrahydrate ($Co(CH_3COO)_2 \cdot 4H_2O$, Sigma-Aldrich), aluminum chloride hexahydrate ($AlCl_3 \cdot 6H_2O$, Merck), and polyvinyl alcohol (PVA, Mw = 72,000, Merck) were used as starting materials without further purification, as commonly employed in electrospun ZnO nanofiber synthesis [14]. A 10 wt% PVA solution was prepared by dissolving PVA in deionized water at 70 °C under continuous stirring for 4 h, followed by aging at room temperature for 8 h to ensure complete polymer chain relaxation and solution homogeneity [7]. Separately, aluminum chloride and cobalt acetate precursor solutions were prepared by dissolving 4 g of each salt in 20 g of deionized water and stirring at 70 °C for 1 h until clear and homogeneous solutions were obtained [10].

The prepared PVA solution was subsequently mixed with the metal salt solutions at a weight ratio of 1:4 and stirred at 70 °C for 8 h to ensure uniform dispersion of metal ions within the polymer matrix. The mixed solution was then stabilized at room temperature for 24 h to improve electrospinnability and solution viscosity stability [16]. As one of the composition variations, the precursor solution with an Al:Co ratio of 100:0 (Al-only,

control sample) was used for the electrospinning process. Electrospinning was carried out using a high-voltage power supply connected to a syringe pump equipped with a stainless-steel needle with an inner diameter of 0.65 mm. The nanofibers were collected on a nonwoven membrane mounted on a rotating drum collector. The electrospinning parameters were optimized and fixed at an applied voltage of 13 kV, a tip-to-collector distance of 13 cm, a solution feed rate of 0.5 mL h^{-1}, and a drum rotation speed of 125 rpm, while the relative humidity was maintained at approximately 58%. These parameters were selected based on previous reports to obtain uniform, bead-free ZnO-based nanofibers [17], [18].

The surface morphology and fiber structure of the electrospun nanofibers were examined using scanning electron microscopy (SEM). The fiber diameter distributions were quantitatively analyzed from SEM micrographs using ImageJ software, and statistical analysis of diameter distribution was performed using Origin software, following established procedures for electrospun nanofiber characterization [19], [20]. The crystalline phase, crystallite size, and degree of crystallinity of the nanofibers were characterized by X-ray diffraction (XRD), which is a standard technique for evaluating structural properties of doped ZnO nanomaterials [21].

RESULT AND DISCUSSION

Morphological Analysis of Electrospun Nanofibers (SEM)

Characterization using Scanning Electron Microscopy coupled with Energy-Dispersive X-ray Spectroscopy (SEM–EDX) was carried out to observe the surface morphology, fiber diameter, and elemental composition of each sample. The microstructural morphology was obtained from SEM analysis by scanning the sample surface using an electron beam at magnifications of 5000×, 10,000×, and 25,000×.

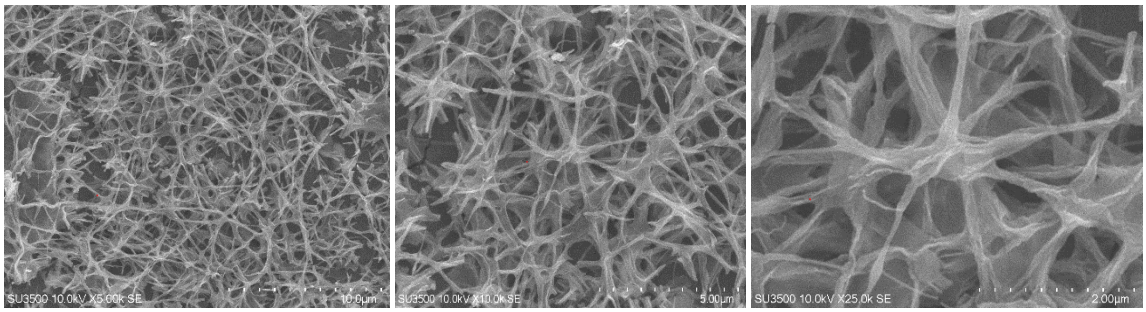

Figure 1. SEM images of the 100% $AlCl_3$ sample at magnifications of (a) 5000×, (b) 10,000×, and (c) 25,000×

The SEM images in Figure 1 show that the 100% $AlCl_3$ sample exhibits a nanofiber structure forming a porous and interwoven network. At magnifications of 5000× to 10,000×, the nanofibers are uniformly distributed without significant agglomeration, indicating that the electrospinning process successfully produced homogeneous fibers with good morphological stability [17], [22]. Such uniform fiber distribution is essential for achieving consistent mechanical deformation and reliable electrical output in piezoelectric applications [3]. At a higher magnification of 25,000×, the surface features of the nanofibers become more pronounced, revealing a relatively rough surface texture. This morphology is commonly observed in polycrystalline ZnO nanofibers after thermal treatment and is considered beneficial for stress transfer under mechanical loading [10]. Based on the SEM scale bar, the nanofiber diameter is estimated to be in the range of 100–200 nm [4]. Nanofibers within this diameter range are known to exhibit enhanced flexibility and strain sensitivity, which are advantageous for piezoelectric nanogenerator applications [3], [23].

In addition to SEM characterization, Energy-Dispersive X-ray (EDX) analysis was carried out to evaluate the elemental composition and distribution within the samples. The EDX results confirm the presence of O, Al, Zn, and Co elements in the samples, indicating successful incorporation of dopant elements into the ZnO nanofiber matrix without detectable impurity phases [24]. Minor deviations between theoretical and experimental values can be attributed to the surface-sensitive nature of EDX analysis and local compositional variations within the nanofibers [25]. The confirmed presence and distribution of Al and Co dopants are crucial, as dopant-induced lattice distortion and defect engineering are known to enhance polarization behavior and piezoelectric performance in ZnO-based nanostructures [10].

Elemental Composition Analysis (EDX)

To provide a more detailed evaluation of the elemental composition of the synthesized nanofibers, Energy-Dispersive X-ray (EDX) analysis was conducted. EDX provides both qualitative and semi-quantitative information regarding elemental composition and is widely used to verify the successful incorporation of dopant elements within oxide nanostructures [24]. The EDX spectra reveal the presence of oxygen (O), zinc (Zn),

aluminum (Al), and cobalt (Co), indicating that the electrospinning and calcination processes successfully produced Al–Co co-doped ZnO nanofibers without the appearance of unintended impurity elements. Table 1 summarizes the comparison between the theoretical weight percentages calculated based on stoichiometric relations and the experimental values obtained from EDX measurements.

The experimental elemental compositions show reasonable agreement with the theoretical values, with minor deviations that can be attributed to instrumental limitations, the surface-sensitive nature of EDX analysis, and local compositional variations within the nanofibers. These results confirm that the electrospinning and subsequent thermal treatment processes effectively preserved the intended chemical composition of the samples. The verified presence of Al and Co dopants is particularly important, as dopant-induced lattice distortion and defect engineering are known to significantly influence charge polarization, crystal symmetry, and piezoelectric response in ZnO-based nanostructures [24], [25]. Such compositional control is therefore essential for optimizing the performance of ZnO-based piezoelectric nanogenerators.

Table 1. EDX analysis results of Al–Co-doped ZnO nanofibers

Element	Weight %	Atomic %	Net int.
O K	11.37	21.54	577.83
Al K	56.57	63.56	4086.36
Co K	0.47	0.24	6.08
Zn K	31.60	14.66	169.72

Based on the EDX results, O, Al, Zn, and Co elements were detected, indicating that the synthesized material consists of metal oxides with the presence of aluminum and cobalt dopants. The absence of other elements suggests relatively good material purity. The dominance of Al and the presence of trace amounts of Co indicate that the doping process was successful. The substitution of Al^{3+} for Zn^{2+} may produce charge imbalance, which can promote the formation of oxygen vacancies and lattice strain. This combination of effects is expected to enhance local polarization and improve the piezoelectric performance of the material.

XRD Analysis: Crystallite Size

In this study, ZnO nanofibers composed of nanoscale crystallites were characterized using X-ray diffraction (XRD) to identify the diffraction peaks and evaluate their crystallographic structure. The diffraction patterns were further analyzed using the HighScore Plus software. The results are shown in Figure 2.

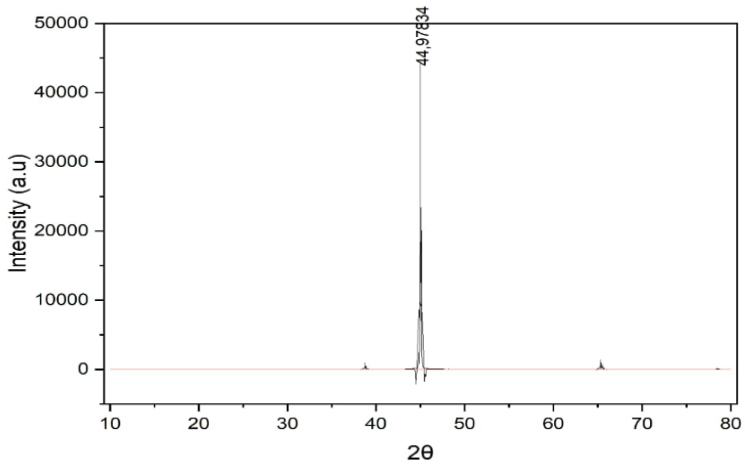

Figure 2. XRD diffraction pattern of Al–Co-doped ZnO nanofibers

The XRD pattern is dominated by a strong diffraction peak corresponding to the (002) plane, while other characteristic ZnO peaks are present with significantly lower intensities with high intensity and a low background, indicating good crystallinity and a preferred crystal orientation of the synthesized ZnO nanofibers [21]. The diffraction peaks can be indexed to the hexagonal wurtzite crystal structure of ZnO, which is consistent with standard JCPDS data and previous reports on ZnO-based nanostructures [26]. The absence of secondary phases or impurity-related peaks further confirms the phase purity of the synthesized materials.

The crystallite size was calculated using the Debye–Scherrer equation based on the full width at half maximum (FWHM) of the diffraction peak. The calculated crystallite size lies in the nanometer range, indicating that each nanofiber consists of an assembly of nanoscale crystallites rather than a single crystal [27]. This structural characteristic is advantageous for piezoelectric applications, as the combination of nanoscale crystallites and one-dimensional nanofiber morphology can enhance mechanical deformation and induce higher local polarization under external stress [28].

In addition, the microstrain (ε), which reflects lattice distortion and defect density, was estimated from the FWHM using the Williamson–Hall approach in its simplified form. The presence of microstrain suggests lattice distortion that may arise from dopant incorporation and size-induced effects, which is known to influence the piezoelectric response of ZnO nanostructures [25]. Referring to the FWHM value, the crystallite size (D) of ZnO samples was calculated using the Debye–Scherrer equation as follows:

$$D = \frac{k\lambda}{\beta \cos\theta} \quad (1)$$

Meanwhile, the microstrain value was calculated using the following equation:

$$\varepsilon = \frac{\beta}{4\,tan\,\theta} \quad (2)$$

Here, k is the Scherrer constant (0.9), λ is the XRD wavelength (0.154056 nm), θ is the diffraction angle, β is the full width at half maximum (FWHM), D is the crystallite size, and ε is the microstrain.

Table 2. Structural parameters of ZnO nanoparticle samples

No.	2θ (°)	h	k	l	FWHM	Crystallite size (nm)	d-spacing (nm)	Microstrain
1	38.739	1	1	1	0.16	84.21	0.281	0.00015
2	43.697	0	0	2	0.14	85.59	0.260	0.00017
3	44.971	0	0	2	0.15	85.98	0.247	0.00018
4	65.316	0	2	2	0.13	94.36	0.191	0.00027
5	78.422	1	1	3	0.12	102.53	0.163	0.00035
6	82.721	1	1	3	0.14	105.84	0.148	0.00038

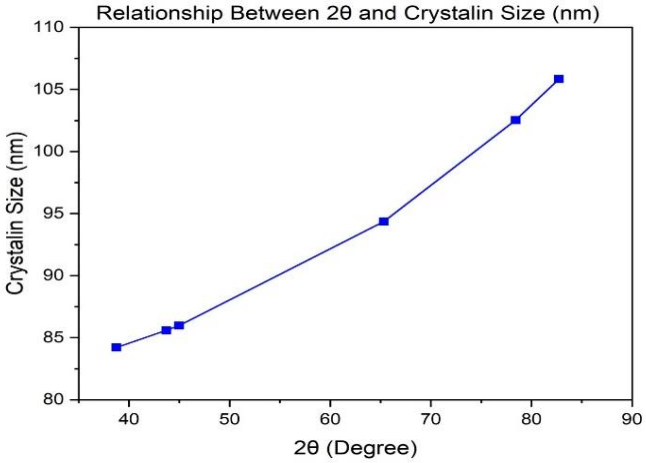

Figure 3. Relationship between 2θ and crystallite size

Based on the XRD results, the crystallite size of the synthesized ZnO ranges from 84 to 106 nm and shows an increasing trend at higher diffraction angles (2θ). The Scherrer equation indicates that peaks at higher 2θ values may yield larger crystallite sizes due to the cosθ term in the equation. The microstrain value also increases from 0.00015 to 0.00038, indicating a slight increase in lattice distortion at higher 2θ values.

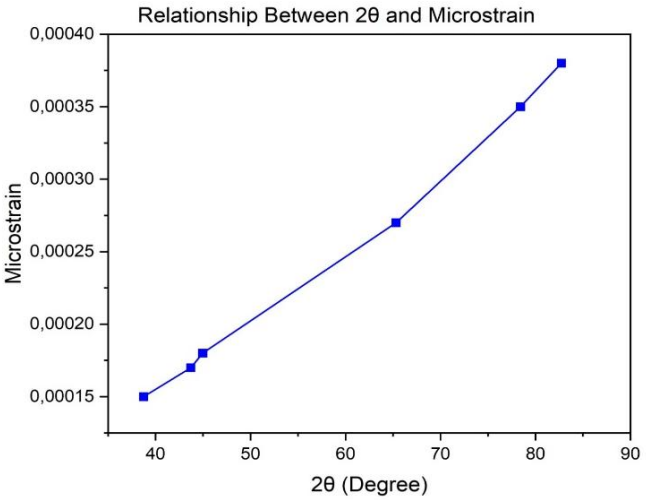

Figure 4. Relationship between 2θ and microstrain

Figure 4 shows the relationship between the diffraction angle 2θ and microstrain in doped ZnO nanofibers. It is observed that the microstrain value increases from 1.5×10^{-4} to 3.8×10^{-4} with increasing 2θ. This increase is attributed to the higher sensitivity of higher-order crystal planes to lattice distortion, as well as local strain effects due to the substitution of Al^{3+} and Co^{2+} ions in the ZnO lattice. Despite the increase in crystallite size, the presence of microstrain indicates residual internal stress, which may enhance local polarization and thus benefit piezoelectric applications.

CONCLUSIONS

Aluminum (Al) and cobalt (Co) co-doped ZnO nanofibers were successfully synthesized, exhibiting a highly interconnected and porous fibrous morphology with uniform distribution and fiber diameters of 100–200 nm. EDX analysis confirmed the presence of O, Zn, Al, and Co without detectable impurities, indicating good material purity and effective dopant incorporation. XRD results revealed a well-defined hexagonal wurtzite crystal structure with high crystallinity and a dominant preferred orientation. The crystallite size ranged from 84 to 106 nm and showed an increasing trend at higher diffraction angles (2θ), while the microstrain increased from 1.5×10^{-4} to 3.8×10^{-4}, indicating lattice distortion induced by Al^{3+} and Co^{2+} substitution. The presence of microstrain is expected to promote local polarization, highlighting the potential of Al–Co co-doped ZnO nanofibers for piezoelectric material development.

ACKNOWLEDGEMENTS

The authors sincerely acknowledge the valuable support and contributions of all parties who assisted in the completion of this research. Special thanks are extended to Politeknik Enjinering Indorama for providing essential equipment used in the characterization process. This research was financially supported by the PDP program, funded by DPPM–DIKTISAINTEK, under Contract No. DIPA 139.04.1.693320/2025.

REFERENCES

[1] A. Janotti and C. G. Van de Walle, “Fundamentals of zinc oxide as a semiconductor,” *Reports Prog. Phys.*, vol. 72, no. 12, p. 126501, 2009, doi: https://doi.org/10.1088/0034-4885/72/12/126501.

[2] C. Jin, J. Zhou, Z. Wu, and J. X. J. Zhang, “Doped Zinc Oxide-Based Piezoelectric Devices for Energy Harvesting and Sensing,” *Adv. Energy Sustain. Res.*, vol. 6, no. 9, p. 2500017, Sep. 2025, doi: https://doi.org/10.1002/aesr.202500017.

[3] Z. L. Wang and J. Song, “Piezoelectric nanogenerators based on zinc oxide nanowire arrays,” *Science*, vol. 312, no. 5771, pp. 242–246, Apr. 2006, doi: https://doi.org/10.1126/science.1124005.

[4] N. Bhadwal, R. Ben Mrad, and K. Behdinan, “Review of Zinc Oxide Piezoelectric Nanogenerators: Piezoelectric Properties, Composite Structures and Power Output,” *Sensors*, vol. 23, no. 8. p. 3859, 2023. doi: https://doi.org/10.3390/s23083859.

[5] S. Xu, Y. Qin, C. Xu, Y. Wei, R. Yang, and Z. L. Wang, “Self-powered nanowire devices,” *Nat. Nanotechnol.*, vol. 5, no. 5, pp. 366–373, May 2010, doi: https://doi.org/10.1038/nnano.2010.46.

[6] E. S. Nour *et al.*, “Low-Frequency Self-Powered Footstep Sensor Based on ZnO Nanowires on Paper Substrate,” *Nanoscale Res. Lett.*, vol. 11, no. 1, p. 156, 2016, doi: https://doi.org/10.1186/s11671-016-1373-1.

[7] H. Parangusan, D. Ponnamma, and M. A. A. Al-Maadeed, “Stretchable Electrospun PVDF-HFP/Co-ZnO Nanofibers as Piezoelectric Nanogenerators,” *Sci. Rep.*, vol. 8, no. 1, p. 754, 2018, doi: https://doi.org/10.1038/s41598-017-19082-3.

[8] C. Klingshirn, “ZnO: material, physics and applications,” *Chemphyschem*, vol. 8, no. 6, pp. 782–803, Apr. 2007, doi: https://doi.org/10.1002/cphc.200700002.

[9] C. Jin *et al.*, “Flexible piezoelectric nanogenerators using metal-doped ZnO-PVDF films,” *Sensors Actuators A Phys.*, vol. 305, p. 111912, 2020, doi: https://doi.org/10.1016/j.sna.2020.111912.

[10] S. Hajer *et al.*, “Influence of (Co+Al) co−doping on structural, micro-structural, optical and electrical properties of nanostructured zinc oxide,” *Ceram. Int.*, vol. 50, no. 21, Part C, pp. 44151–44164, 2024, doi: https://doi.org/10.1016/j.ceramint.2024.08.264.

[11] R. Saleh and N. F. Djaja, “Transition-metal-doped ZnO nanoparticles: Synthesis, characterization and photocatalytic activity under UV light,” *Spectrochim. Acta Part A Mol. Biomol. Spectrosc.*, vol. 130, pp. 581–590, 2014, doi: https://doi.org/10.1016/j.saa.2014.03.089.

[12] C. Liu *et al.*, “Improvement in the Piezoelectric Performance of a ZnO Nanogenerator by a Combination of Chemical Doping and Interfacial Modification,” *J. Phys. Chem. C*, vol. 120, no. 13, pp. 6971–6977, Apr. 2016, doi: https://doi.org/10.1021/acs.jpcc.6b00069.

[13] D. Subagiyo and Suyitno, “Enhancing Output Voltage of Piezoelectric-Based Nanogenerators Using Zinc Oxide

Material Codoped with Aluminum and Cobalt," *IOP Conf. Ser. Mater. Sci. Eng.*, vol. 267, no. 1, p. 12037, 2017, doi: https://doi.org/10.1088/1757-899X/267/1/012037.

[14] S. Ramakrishna, K. Fujihara, W.-E. Teo, T.-C. Lim, and Z. Ma, *An Introduction to Electrospinning and Nanofibers*. World Scientific, 2005. doi: https://doi.org/10.1142/5894.

[15] X. Li *et al.*, "From Fiber to Power: Recent Advances Toward Electrospun-Based Nanogenerators," *Adv. Funct. Mater.*, vol. 35, no. 13, p. 2418066, Mar. 2025, doi: https://doi.org/10.1002/adfm.202418066.

[16] T. Pirzada, S. A. Arvidson, C. D. Saquing, S. S. Shah, and S. A. Khan, "Hybrid Silica–PVA Nanofibers via Sol–Gel Electrospinning," *Langmuir*, vol. 28, no. 13, pp. 5834–5844, Apr. 2012, doi: https://doi.org/10.1021/la300049j.

[17] A. Greiner and J. H. Wendorff, "Electrospinning: A Fascinating Method for the Preparation of Ultrathin Fibers," *Angew. Chemie Int. Ed.*, vol. 46, no. 30, pp. 5670–5703, Jul. 2007, doi: https://doi.org/10.1002/anie.200604646.

[18] B. A. Chinnappan, M. Krishnaswamy, H. Xu, and M. E. Hoque, "Electrospinning of Biomedical Nanofibers/Nanomembranes: Effects of Process Parameters," *Polymers*, vol. 14, no. 18. p. 3719, 2022. doi: https://doi.org/10.3390/polym14183719.

[19] J. Schindelin *et al.*, "Fiji: an open-source platform for biological-image analysis," *Nat. Methods*, vol. 9, no. 7, pp. 676–682, 2012, doi: https://doi.org/10.1038/nmeth.2019.

[20] C. A. Schneider, W. S. Rasband, and K. W. Eliceiri, "NIH Image to ImageJ: 25 years of image analysis," *Nat. Methods*, vol. 9, no. 7, pp. 671–675, 2012, doi: https://doi.org/10.1038/nmeth.2089.

[21] B. D. Cullity and S. R. Stock, *Elements of X-ray Diffraction*, 3rd ed. United States: Pearson, 2014.

[22] P. Fakhri *et al.*, "Flexible hybrid structure piezoelectric nanogenerator based on ZnO nanorod/PVDF nanofibers with improved output," *RSC Adv.*, vol. 9, no. 18, pp. 10117–10123, 2019, doi: http://dx.doi.org/10.1039/C8RA10315A.

[23] C.-L. Hsu and K.-C. Chen, "Improving Piezoelectric Nanogenerator Comprises ZnO Nanowires by Bending the Flexible PET Substrate at Low Vibration Frequency," *J. Phys. Chem. C*, vol. 116, no. 16, pp. 9351–9355, Apr. 2012, doi: 10.1021/jp301527y.

[24] J. I. Goldstein, D. E. Newbury, J. R. Michael, N. W. M. Ritchie, J. H. J. Scott, and D. C. Joy, *Scanning Electron Microscopy and X-Ray Microanalysis*. New York, NY: Springer, 2018. doi: http://doi.org/10.1007/978-1-4939-6676-9.

[25] A. R. West, *Solid State Chemistry and its Applications*, 2nd ed. Chichester: John Wiley & Sons, Ltd., 2014.

[26] Ü. Özgür *et al.*, "A comprehensive review of ZnO materials and devices," *J. Appl. Phys.*, vol. 98, no. 4, p. 41301, Aug. 2005, doi: https://doi.org/10.1063/1.1992666.

[27] A. L. Patterson, "The Scherrer Formula for X-Ray Particle Size Determination," *Phys. Rev.*, vol. 56, no. 10, pp. 978–982, Nov. 1939, doi: https://doi.org/10.1103/PhysRev.56.978.

[28] Y. Qin, X. Wang, and Z. L. Wang, "Microfibre–nanowire hybrid structure for energy scavenging," *Nature*, vol. 451, no. 7180, pp. 809–813, 2008, doi: https://doi.org/10.1038/nature06601.